Optical parametric oscillator pumped by femtosecond Yb-doped fiber laser

Keisuke Nagashima

Ultrafast Dynamics Group, Department of Advanced Photon Research

A synchronously pumped optical parametric oscillator (SPOPO) is a powerful tool for generating femtosecond and picosecond pulses. However, the pulse energies are on the order of nanojoules because of the high repetition frequency of several tens of megahertz. Higher pulse energies are needed and considerable work has been reported for increasing SPOPO pulse energies [1–8]. Here, we report the first demonstration of an SPOPO pumped by a femtosecond Yb-doped fiber laser operated in a burst mode. The burst-mode operation increases the pulse energy by limiting the total number of pulses [9–13].

We developed a Yb-doped fiber laser that featured chirped pulse amplification at a repetition rate of 100 kHz. Figure 1 shows the laser system, which consists of a mode-locked fiber oscillator, a pulse stretcher, a fiber pre-amplifier, a Pockels cell, multi-stage fiber amplifiers, and a pulse compressor.

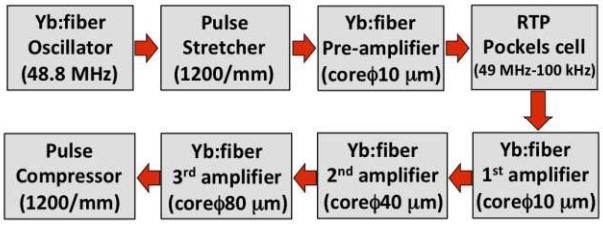

Fig. 1. Block diagram of the Yb-doped fiber laser system.

The repetition frequency of the mode-locked fiber oscillator was 48.8 MHz. Femtosecond pulses generated in the oscillator were stretched in the pulse stretcher and amplified in the pre-amplifier. Then, the repetition frequency was reduced from 48.8 MHz to 100 kHz by the Pockels cell (RTP-4-20, LEYSOP). The 100 kHz pulses were amplified in three-stage fiber amplifiers and were compressed in the pulse compressor. The core diameters of the Yb-doped fibers were 10 μm, 40 μm, and 80 μm in the three-stage amplifiers. Gold-coated 1200 groove/mm reflection gratings were used in both the pulse stretcher and pulse compressor. Self-phase modulation in the fibers was minimized by controlling the laser-diode pump power for each amplifier. The output pulses had a central wavelength of 1039 nm, a full-width at half-maximum (FWHM) spectral width of 7 nm, and a FWHM pulse length of 350 fs. The output power from the final amplifier was limited up to 2.5 W in the experiments.

Periodically poled materials have been used in many SPOPO experiments. They are MgO-doped periodically poled $LiTaO_3$ (MgO:PPLT) and MgO-doped periodically poled $LiNbO_3$ (MgO:PPLN). These materials offer several advantages for increasing pulse energy, such as high nonlinear coefficients and no spatial walk-off that can increase the nonlinear interaction length. MgO:PPLT was used here because it has a high tolerance to optical damage [14].

Figure 2 shows the optical configuration of the SPOPO, in which a fan-out MgO:PPLT crystal was used. The crystal was 1 mol% MgO-doped stoichiometric PPLT (manufactured by OXIDE). The crystal surfaces had broadband anti-reflection coatings for the range of 1000–1700 nm. The crystal had a 11 mm length (propagation direction), a 2 mm height, and a 7 mm width. The effective width was 5 mm, where the poling period had a fan-out structure and changed over range of 29.3–32.4 μm. The dichroic mirror and the spherical lens were CaF_2 to prevent idler light absorption. The dichroic mirror had a transmission band of 1000–1100 nm and a reflection band of 1250–1700 nm. The output coupler had a constant transmission rate of 70% over the 1300–1700 nm range.

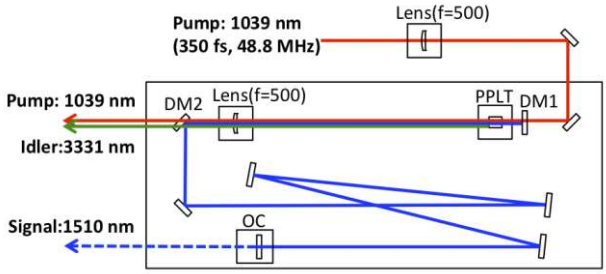

Fig. 2. SPOPO optical configuration. PPLT: MgO:PPLT crystal; DM1 and DM2: dichroic mirrors; OC: output coupler.

The SPOPO had an optical cavity length of 3.07 m, which gives a 48.8 MHz repetition frequency. The ends of the cavity were a dichroic mirror (DM1) and an output coupler (OC). In the cavity design, the signal light had a 0.18 mm radius at the DM1 and a 1.0 mm radius at the OC. The MgO:PPLT crystal was placed in the immediate vicinity of the DM1.

In the experiments, the signal wavelength was tunable in the range of 1450–1700 nm. We adjusted the signal wavelength to 1510 nm, which was generated in coincidence with the 3331 nm idler wavelength. The corresponding poling period of the MgO:PPLT was 30.3 μm. In the crystal, the group indices at the signal, idler, and pump wavelengths were 2.161, 2.193, and 2.185, respectively [15]. Therefore, the signal pulse was faster than the pump pulse and, conversely, the idler pulse was slower than the pump pulse. We used the 11 mm long MgO:PPLT crystal because the interaction length for the parametric conversion increased with crystal length.

The pump and signal pulses were respectively measured by the Si photo-detector with a 0.35 GHz bandwidth and the InGaAs photo-detector with a 5 GHz bandwidth. The sampling frequency of the oscilloscope was 10 GHz for both detectors. Figures 3(b) and (c) show the waveforms of the pump and signal pulses during SPOPO operation. The number of pump pulses was $N = 5$ and the average pump power was 1.7 W. The horizontal axis started from the 100 kHz oscilloscope trigger. The fifth pump pulse was at $t =$ 124 ns and the fifth signal pulse was at $t = 145$ ns. The first signal pulse was not observed and the second was barely detected at $t =$ 83 ns.

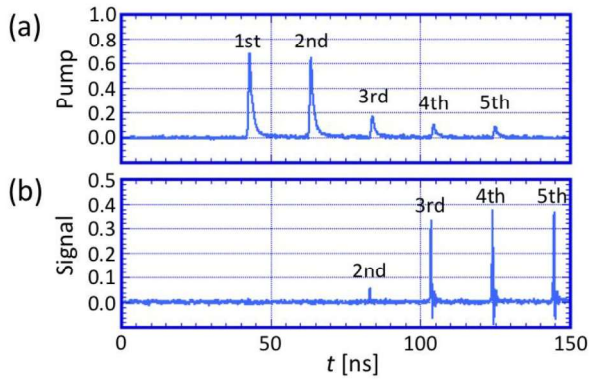

Fig. 3. Waveforms of the pump and signal pulses with SPOPO operation with $N = 5$: (a) pump pulses and (b) signal pulses.

Figure 4(a) shows the fifth signal pulse energy E_{sig} as a function of the pump pulse energy E_{pump}. These pulse energies were measured by the photo-detectors, which were calibrated by power-meters. We generated a signal pulse with energy greater than 1 μJ when $E_{pump} > 2.4$ μJ, and the energy was 1.5 μJ when $E_{pump} = 4.8$ μJ. This is the highest pulse energy reported for femtosecond pulses obtained from an SPOPO. The energy efficiency E_{sig}/E_{pump} was 38% at $E_{pump} = 3.4$ μJ and 32% at $E_{pump} = 4.8$ μJ. The maximum pump intensity on the crystal was 8.3 GW/cm^2, which was considerably lower than that in a previous experiment with a high pump intensity on MgO:PPLN [16]. We observed no damage in the crystal and no parametric generation except for the SPOPO signal.

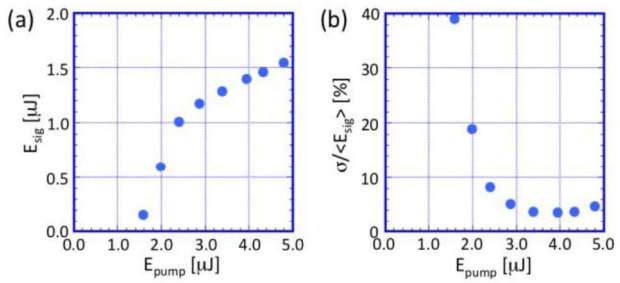

Fig. 4. (a) Energy of the fifth signal pulse as a function of the pump pulse energy. (b) Standard deviation divided by the average value of the signal pulse energy as a function of the pump pulse energy.

Figure 4(b) plots pulse-to-pulse energy fluctuations of the fifth signal pulses as a function of the pump pulse energy E_{pump}. Here, we use the average value of the fifth signal pulse energy as $\langle E_{sig} \rangle$ and the standard deviation as σ. We use the value of $\sigma/\langle E_{sig} \rangle$ as an indicator of the pulse-to-pulse fluctuation. (The pulse-to-pulse fluctuation of the pump pulses was approximately 1%.) This fluctuation was caused by the optical parametric noise, which becomes a seed of the signal pulse. The statistical properties of the signal pulse fluctuation were described in our most recent report [17].

In summary, we demonstrated an SPOPO pumped by a burst-mode Yb-doped fiber laser, which had 100 kHz pulse trains with a finite number of pump pulses that could be controlled by a Pockels-cell gate. We obtained a signal pulse energy of 1.5 μJ with a 4.8-μJ pump pulse. Pulse-to-pulse fluctuations could be suppressed for as few as five pump pulses.

Acknowledgments

The authors thank M. Maruyama and M. Tsubouchi for their support, and T. Otobe, N. Ishii, T. Endo, and H. Akagi for their valuable discussions.

References

1. T. P. Lamour, L. Kornaszewski, J. H. Sun, and D. T. Reid, Opt. Express **17**, 14229 (2009).
2. T. Südmeyer, E. Innerhofer, F. Brunner, R. Paschotta, T. Usami, H. Ito, S. Kurimura, K. Kitamura, D. C. Hanna, and U. Keller, Opt. Lett. **29**, 1111 (2004).
3. F. Kienle, P. S. Teh, S.-U. Alam, C. B. E. Gawith, D. C. Hanna, D. J. Richardson, and D. P. Shepherd, Opt. Lett. **35**, 3580 (2010).
4. T. Petersen, J. D. Zuegel, and J. Bromage, Opt. Express **25**, 8840 (2017).
5. C.-K. Min and T. Joo, Opt. Lett. **3**0, 1855 (2005).
6. L. Xu, H.-Y. Chan, S.-U. Alam, D. J. Richardson, and D. P. Shepherd, Opt. Lett. **40**, 3288 (2015).
7. T. P. Lamour and D. T. Reid, Opt. Express **19**, 17557 (2011).
8. L.-J. He, K. Liu, Y. Bo, Z. Liu, X.-J. Wang, F. Yang, L. Yuan, Q.-J. Peng, D.-F. Cui, and Z.-Y. Xu, Opt. Lett. **43**, 539 (2018).
9. H. Kalaycioglu, K. Eken, and F. O. Ilday, Opt. Lett. **36**, 3383 (2011).
10. H. Kalaycioglu, Y. B. Eldeniz, O. Akçaalan, S. Yava¸s, K. Gürel, M. Efe, and F. O. Ilday, Opt. Lett. **37**, 2586 (2012).
11. X. Li, S. Zhang, Y. Hao, and Z. Yang, Opt. Express **22**, 6699 (2014).
12. H. Kalaycioglu, O. Akçaalan, S. Yava¸s, Y. B. Eldeniz, and F. O. Ilday, J. Opt. Soc. Am. B **32**, 900 (2015).
13. P. Elahi, S. Yilmaz, Y. B. Eldeniz, and F. O. Ilday, Opt. Lett. **39**, 236 (2014).
14. N. E. Yu, S. Kurimura, Y. Nomura, and K. Kitamura, Jpn. J. Appl. Phys. **43**, L1265 (2004).
15. M. Nakamura, S. Higuchi, S. Takekawa, K. Terabe, Y. Furukawa, and K. Kitamura, Jpn. J. Appl. Phys. **41**, L465 (2002).
16. Y. Deng, A. Schwarz, H. Fattahi, M. Ueffing, X. Gu, M. Ossiander, T. Metzger, V. Pervak, H. Ishizuki, T. Taira, T. Kobayashi, G. Marcus, F. Krausz, R. Kienberger, and N. Karpowicz, Opt. Lett. **37**, 4973 (2012).
17. K. Nagashima, Y. Ochi, and R. Itakura, J. Opt. Soc. Am. B **36**, 3389 (2019).